Neumeyer, J., Barthelmes, F., Dierks, O., Flechtner, F., Harnisch, M., Harnisch, G., Hinderer, J., Imanishi, Y., Kroner, C., Meurers, B., Petrovic, S., Reigber, Ch., Schmidt, R., Schwintzer, P., Sun, H.-P., Virtanen, H. (2006): Combination of temporal gravity variations resulting from superconducting gravimeter (SG) recordings, GRACE satellite observations and global hydrology models. - Journal of Geodesy, 79, 10-11, 573-585

DOI: 10.1007/s00190-005-0014-8.

Combination of temporal gravity variations resulting from superconducting gravimeter (SG) recordings, GRACE satellite observations and global hydrology models

J. Neumeyer - F. Barthelmes - O. Dierks - F. Flechtner
M. Harnisch - G. Harnisch - J. Hinderer - Y. Imanishi
C. Kroner - B. Meurers - S. Petrovic - Ch. Reigber
R. Schmidt - P. Schwintzer - H.-P. Sun - H. Virtanen

Abstract Gravity recovery and climate experiment (GRACE)-derived temporal gravity variations can be resolved within the μgal (10^{-8} m/s^2) range, if we restrict the spatial resolution to a half-wavelength of about 1,500 km and the temporal resolution to 1 month. For independent validations, a comparison with ground gravity measurements is of fundamental interest. For this purpose, data from selected superconducting gravimeter (SG) stations forming the Global Geodynamics Project (GGP) network are used. For comparison, GRACE and SG data sets are reduced for the same known gravity effects due to Earth and ocean tides, pole tide and atmosphere. In contrast to GRACE, the SG also measures gravity changes due to load-induced height variations, whereas the satellite-derived models do not contain this effect. For a solid spherical harmonic decomposition of the gravity field, this load effect can be modelled using degree-dependent load Love numbers, and this effect is added to the satellite-derived models. After reduction of the known gravity effects from both data sets, the remaining part can mainly be assumed to represent mass changes in terrestrial water storage. Therefore, gravity variations derived from global hydrological models are applied to verify the SG and GRACE results. Conversely, the hydrology models can be checked by gravity variations determined from GRACE and SG observations. Such a comparison shows quite a good agreement between gravity variation derived from SG, GRACE and hydrology models, which lie within their estimated error limits for most of the studied SG locations. It is shown that the SG gravity variations (point measurements) are representative for a large area within the μgal accuracy, if local gravity effects are removed. The individual discrepancies between SG, GRACE and hydrology models may give hints for further investigations of each data series.

Keywords Superconducting gravimetry · Gravity recovery and climate experiment (GRACE) · Temporal gravity variations · Hydrology models · Cross validation

P. Schwintzer has deceased.

J. Neumeyer · F. Barthelmes · O. Dierks · F. Flechtner · S. Petrovic
Ch. Reigber · R. Schmidt · P. Schwintzer
GeoForschungsZentrum Potsdam,
Dept.1: Geodesy and Remote Sensing,
Telegrafenberg, 14473 Potsdam, Germany,
E-mail: neum@gfz-potsdam.de
E-mail: bar@gfz-potsdam.de
E-mail: dierks@gfz-potsdam.de
E-mail: flechtne@gfz-potsdam.de
E-mail: sp@gfz-potsdam.de
E-mail: reigber@gfz-potsdam.de
E-mail: rschmidt@gfz-potsdam.de
Tel.: +49-331-2881101/1135
Fax: +49-331-2881111

M. Harnisch · G. Harnisch
Federal Agency for Cartography and Geodesy,
Bergblick 12, 14558 Nuthetal, Germany,
E-mail: gmharnisch@t-online.de

J. Hinderer
École et Observatoire des Sciences de la Terre,
Institut de Physique du Globe de Strasbourg,
5 rue Descartes, 67084 Strasbourg Cedex, France
E-mail: Jacques.Hinderer@eost.u-strasbg.fr

Y. Imanishi
Ocean Research Institute Tokyo,
1-15-1, Minamidai, Nakano, Tokyo 164-8639, Japan
imanishi@ori.u-tokyo.ac.jp

C. Kroner
Institute of Geosciences, Friedrich Schiller University of Jena,
Burgweg 11, 07749 Jena, Germany
corinna.kroner@uni-jena.de

B. Meurers
Institute of Meteorology and Geophysics,
University of Vienna,
Althanstrasse 14, 1090 Wien, Austria
bruno.meurers@univie.ac.at

H.-P. Sun
Institute of Geodesy and Geophysics,
Chinese Academy of Sciences,
174 Xu-Dong Road, 430077 Wuhan, People Republic of China
heping@asch.whigg.ac.cn

H. Virtanen
Finnish Geodetic Institute,
P.O. Box 15 (Geodeetinrinne 2), 02431 Masala, Finland
heikki.virtanen@fgi.fi

1 Introduction

One objective of the new-generation GRACE (gravity recovery and climate experiment) (e.g. Tapley and Reigber 2001) satellite gravity mission is the recovery of temporal Earth gravity field variations. The results of a recent GRACE data evaluation show a gravity resolution in the μgal range at a half-wavelength ($\lambda/2$) spatial resolution of about 1,500 km for a temporal resolution of 1 month (Schmidt et al. 2005a). Because of this remarkable gravity resolution, the comparison and validation of satellite-derived temporal gravity variations with ground gravity measurements is of fundamental interest. A proposal for such a comparison was made by Crossley and Hinderer (2002) and Crossley et al. (2003).

The time variation contained in the GRACE solutions ranges from 1 month to the lifetime of GRACE (20 months in this study). Therefore, surface gravity measurements must have a long-term stability, which only superconducting gravimeters (SG) (Goodkind 1999) fulfil. As such, the aim of the comparison presented in this paper is as follows: validation of the GRACE results, checking of the SG data pre-processing and reduction procedures and checking of gravity variations derived from hydrological models.

On the Earth's surface, high-precision gravity measurements are carried out with SG's of the Global Geodynamics Project (GGP) network (Crossley et al. 1999). These measurements have a gravity resolution of about 0.1 μgal in the time domain (reaching 1 ngal [10^{-11} m/s^2] in the tidal band by integration over 2 or 3 years) and a linear drift of some μgal per year. The gravity resolution of the SG measurements is frequency-dependent. It decreases for longer periods, mainly caused by the noise at the site (Rosat et al. 2004) and the reduction quality of environmental gravity effects induced by atmosphere and hydrosphere.

For comparison of satellite-derived with ground-measured temporal gravity variations, we must be sure to the best knowledge that, after pre-processing and reduction of known gravity effects, both data sets represent the same sources of gravitation at the same spatial resolution. Particularly the spatial resolution raises some questions because the SG measurements are merely point measurements. How representative are these for an area with the extent of approximately 1,500 km, which is the spatial resolution of the GRACE satellite-derived temporal gravity variation?

The first comparison between temporal gravity variations derived from SG and CHAMP has shown a noticeable agreement (Neumeyer et al. 2004a). It could be inferred that the SG gravity variations are valid for a large area within the μgal accuracy, if the local gravity effects are carefully removed. Further studies confirm the quality of gravity field variation measurements with SGs in Europe (Crossley et al. 2005). With the increased gravity and spatial resolution of GRACE solutions (Reigber et al. 2005; Schmidt et al. 2005a), this kind of comparison can be studied in more detail. Eight stations have been chosen from the global SG GGP network, which cover a large test field and also allow studying of closely located SG stations. These are:

- Sutherland/South Africa (SU): $\varphi = -32.381°$, $\lambda = 20.811°$, $h = 1791$ m
- Moxa/Germany (MO): $\varphi = 50.645°$, $\lambda = 11.616°$, $h = 455$ m
- Wettzell/Germany (WE): $\varphi = 49.144°$, $\lambda = 12.878°$, $h = 580$ m
- Strasbourg/France (ST): $\varphi = 48.622°$, $\lambda = 7.684°$, $h = 180$ m
- Vienna/Austria (VI): $\varphi = 48.249°$, $\lambda = 16.358°$, $h = 192.4$ m
- Metsahovi/Finland (ME): $\varphi = 60.217°$, $\lambda = 24.396°$, $h = 56$ m
- Wuhan/China (WU): $\varphi = 30.516°$, $\lambda = 114.49°$, $h = 80$ m
- Matsushiro/Japan (MA): $\varphi = 36.543°$, $\lambda = 138.207°$, $h = 406$ m

The following data sets were used for this study: GRACE monthly gravity field solutions, SG recordings, 3D air pressure variations, groundwater level variations measured at SG sites and gravity variations derived from hydrology models within the time period from April 2002 to November 2003.

2 Accuracy of gravity signals derived from GRACE, SG and hydrology models

The recovery of GRACE-derived gravity variations is based on monthly averages of time-varying gravitational potential (see Sect. 4.1). Reigber et al. (2005) describe the determination of the gravity field models from GRACE data. The formal error estimates were a posteriori calibrated based on the scattering of subset solutions.

A special method for calibrating the formal errors of monthly solutions is described in Schmidt et al. (2005a). Figure 1 shows these calibrated errors of the monthly solutions with increasing degree ℓ of the spherical harmonic coefficients. With higher degree ℓ, the spatial resolution becomes finer ($\lambda/2 \approx 2 \cdot 10^4/\ell$), but the error increases. A comparison of the calibrated errors of the monthly GRACE solutions with the signal amplitudes of the monthly hydrology model-derived gravity variations shows that the cumulated error (dotted lines in Fig. 1) equals the hydrology signal at about degree ℓ=16 and the error per degree (solid lines in Fig. 1) equals the hydrology signal per degree at ℓ=10. Thus, to ensure that the GRACE errors are smaller than the expected hydrology effect, we used the GRACE and hydrology models up to a maximum degree of $\ell_{\max}$=10 for comparison. Table 1 roughly summarizes the GRACE parameters for a spatial resolution of 500 and 2000 km in comparison with the SG.

3 Preconditions for combining satellite-derived and ground-measured temporal gravity variations

A combination of satellite-derived with ground-measured temporal gravity variations requires representative data sets

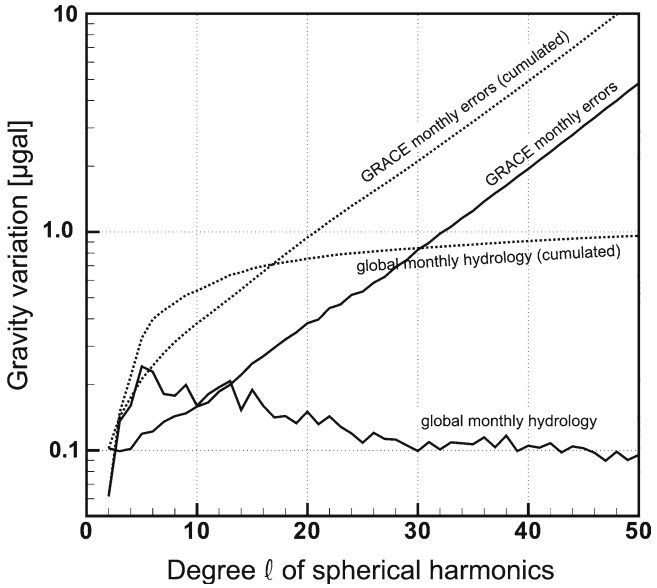

Fig. 1 Calibrated errors of Gravity recovery and climate experiment (GRACE) monthly solutions and gravity variations derived from the Water gap Global Hydrology Model (WGHM) as functions of degree ℓ of spherical harmonics. Monthly solutions per degree (*solid line*) and monthly solutions as function of maximum degree (*dotted*)

Table 1 Performance parameters of Gravity recovery and climate expreiment (GRACE) and superconducting gravimeter (SG)

	GRACE		SG
Gravity resolution (μgal)	10	0.5	0.1
Spatial resolution $\lambda/2$	500 km	2,000 km	Point
Spherical Harmomic coefficient	ℓ_{max}=40	ℓ_{max}=10	N/a
Temporal resolution	1 month		10 s
Long-term stability (drift)	No drift		$\sim$3 μgal/year

with the same sources of gravitation and comparable spatial resolutions. This can be achieved by:

- Reduction of the same known gravity effects in both data sets using the same models
- Adaptation of the SG gravity variations to the spatial resolution of the satellite
- Consideration of effects that are unique to each method.

On the Earth's surface, the SG measures, besides the gravitational mass attraction, the gravity effect due to elastic deformation (vertical surface shift) (e.g. Pick et al. 1973; Vaníček and Krakiwsky 1982) and the deformation potential (mass redistribution due to vertical surface shift). In contrast to the SG, the satellite is not coupled to the Earth's surface and thus it is only sensitive to the change in gravitational potential. The part that comes from the fact that the SG has changed its location due to the deformation is sensed by SG only. The reductions of Earth and pole tide, and also the loading effects of atmosphere and hydrosphere, are different for SG and GRACE. Body Love numbers h_ℓ and load Love numbers h'_ℓ, which describe the height variations, are only relevant for the SG data processing.

The spatial resolution for the remaining gravity variations after reduction of the known effects is different for SG (point measurements) and GRACE (spatial resolution of $\lambda/2$ between 1,000 and 2,000 km used in this study). The SG measurements include gravity variations from short- to long-periodic spatial distribution. For comparison, only the gravity variations related to the spatial resolution of GRACE should be taken into account. The present way for adapting the remaining SG gravity variations to the spatial resolution of GRACE consists in removing the local gravity effects, mainly induced by the hydrology, from SG data.

4 Preparing the gravity variations for comparison

Before comparing SG and GRACE gravity variations, the SG measurements must be reduced for the same gravity effects that have been applied in the GRACE data processing. These effects are:

1. Earth tides
2. Pole tide
3. Gravity variations induced by the atmosphere
4. Ocean tidal loading.

The same models are used for both sets of gravity variations to reduce these effects. Additionally, the load-induced height variations, contained in the SG measurements, are added to the monthly GRACE solutions (see Sect. 4.1).

4.1 Monthly gravity field solutions from GRACE

Monthly batches of GRACE science instrument data were collected to recover monthly averages of the time-varying gravitational potential. The observations provided by the on-board instruments are GPS-GRACE high–low satellite-to-satellite (hl-SST) carrier-phase differences and code pseudo-ranges from the GPS BlackJack receivers, non-conservative accelerations from the SuperSTAR accelerometers, attitude angles from the star cameras and low–low satellite-to-satellite (ll-SST) rates of distance changes from the K-band intersatellite link. The instrumentation and on-board instrument processing units are described in detail in Dunn et al. (2003).

The process of global gravity field recovery from GRACE data, as applied at GeoForschungsZentrum Potsdam (GFZ) using its Earth parameter and orbit estimation system (EPOS), is described in detail, together with the mean field solution EIGEN-GRACE02S, in Reigber et al. (2005). The computation of the monthly gravity field solutions is described in Schmidt et al. (2005b).

As for EIGEN-GRACE02S, the Stokes coefficients of a spherical harmonic expansion of the gravitational potential were adjusted up to degree and order 150 for each of the monthly gravity field solutions, exploiting GRACE data for a particular calendar month. During creation of the normal

equation systems, several time-varying gravitational phenomena are accounted for in the underlying dynamic model. These are:

- Earth tides and pole tide: Determined according to International Earth Rotation Service (IERS) Conventions 2003 (McCarthy and Petit 2004). The pole tide is based on the IERS polar motion series. The recording of the polar motion is carried out with very long baseline interferometry (VLBI), lunar laser ranging (LLR), satellite laser ranging (SLR) and GPS measurements. IERS provides a smoothing of these measurements with a resolution of 1 day (Bulletin B).
- Atmospheric attraction and loading: For atmosphere de-aliasing, atmospheric pressure grids at different altitudes available at six-hour intervals from the European Centre for Medium-Range Weather Forecast (ECMWF) are evaluated by vertical integration (Flechtner 2003b).
- Ocean tidal loading: Applying the FES2002 ocean tidal model (Le Provost et al. 2002) supplemented by long-period tides (Lyard (1998). For ocean de-aliasing, a barotropic model (Ali and Zlotnicki 2003) is used to estimate the non-tidal ocean mass variability at the same intervals. The ocean pole tide (Desai 2002; Chen et al. 2004) is not considered.
- Changes in potential caused by post-glacial rebound: In addition to a linear drift in C20 (IERS Conventions 2003) secular variations in the zonals of degrees 3 and 4 (Cheng et al. 1997) were included in the a priori modelling during the gravity recovery process.

Atmospheric and ocean mass contributions are summed up to yield a time-series of corrections in terms of gravitational spherical harmonic coefficients up to degree and order 50 with a 6-h interval. The corrections are added to the initial mean gravitational potential when computing the satellite's gravitational accelerations for dynamic orbit and gravity field parameter adjustment. However, besides the accuracy of the atmospheric and oceanic models used, aliasing effects can further deteriorate the quality of the applied corrections (see Thompson et al. 2004). According to Han et al. (2004), the degree-error relative to the measurement error is increased by a factor of ∼20 due to atmospheric aliasing and by a factor of ∼10 due to oceanic aliasing.

With these background models in mind, the differences between monthly gravity field solutions should reflect, apart from instrumental noise, residual mismodelling in tidal and non-tidal atmosphere and ocean variability, and unmodelled longer-term variations, mainly continental hydrological phenomena including ice shield mass variations.

The GRACE products were developed, processed and archived in the Science Data System (SDS) (available at the GFZ Information System and Data Center [ISDC] http://isdc.gfz-potsdam.de/grace), which is shared among the Jet Propulsion Laboratory (JPL), the University of Texas Center for Space Research [UTCSR] and the GFZ Potsdam. For comparison, we also used the available GRACE monthly solutions from UTCSR. Although the solutions of SDS centres at UTCSR and GFZ use the same GRACE instrument database (Level-1B data provided by JPL) and the dynamic method for orbit determination and gravity recovery, results for the estimated monthly gravity fields differ as revealed in Fig. 5 (shown later). These differences may originate from various sources within the processing standards. Details related to all of these items can be found in the Level-2 Processing Standards Documents for UTCSR (Bettadpur 2004) and GFZ (Flechtner 2003a). Further information on the GFZ processing strategy can be found in Reigber et al. (2005).

In addition to the direct gravity field variations, the SG also measures the gravity changes due to the load-induced variations of the radial position of the SG, whereas the satellite-derived models naturally do not contain this effect. If we have a spherical harmonic decomposition of the gravity field, this load effect can be modelled using the degree-dependent load Love numbers h_ℓ' (Farrell 1972, Zürn and Wilhelm 1984, Hinderer and Legros 1989). Therefore, we will add this effect to the satellite-derived models. The associated satellite-derived gravitational potential is:

$$W(r,\varphi,\lambda) = \frac{GM}{R}\sum_{\ell=0}^{\ell\max}\left(\frac{R}{r}\right)^{\ell+1}\sum_{m=0}^{\ell}\left[\bar{C}_{\ell m}\cdot\cos(m\lambda) + \bar{S}_{\ell m}\cdot\sin(m\lambda)\right]\cdot\bar{P}_{\ell m}(\sin\varphi) \quad (1)$$

where r, φ, λ are the spherical geocentric coordinates of the computation point (radius, longitude, latitude), R is the reference radius (mean equatorial radius of the Earth), GM is the gravitational constant times mass of the Earth, ℓ, m are degree and order of the spherical harmonics, $\ell_{\max}$ is the chosen maximum degree in practical calculations (any natural number, $\ell_{\max} < \infty$), $\overline{P}_{\ell m}$ are the fully normalized Legendre functions, and $\overline{C}_{\ell m}, \overline{S}_{\ell m}$ are the fully normalized Stokes coefficients.

The variation of the gravity field in time with respect to some mean field is then derived as variation $\delta\overline{C}_{\ell m}, \delta\overline{S}_{\ell m}$ of the coefficients. The variation δr of the radial position of the SG caused by the variation of the geoid height ∂N_ℓ, which is the variation of the Earth's equilibrium figure, can be described by:

$$\delta r = \sum_{\ell=0}^{\ell\max}\delta r_\ell = \sum_{\ell=0}^{\ell\max}\delta N_\ell\cdot h_\ell' \quad (2)$$

where δN_ℓ is the geoid variation of degree ℓ of its spherical harmonic decomposition.

In spherical approximation (Heiskanen and Moritz 1967), the geoid height variation at the point (φ, λ) can be represented by:

$$\delta N(\varphi,\lambda) = \sum_{\ell=0}^{\ell\max}\delta N_\ell = R\cdot\sum_{\ell=0}^{\ell\max}\sum_{m=0}^{\ell}\left[\delta\bar{C}_{\ell m}\cdot\cos(m\lambda) + \delta\bar{S}_{\ell m}\cdot\sin(m\lambda)\right]\cdot\bar{P}_{\ell m}(\sin\varphi) \quad (3)$$

The corresponding gravity variation detected by the satellite in spherical approximation is:

$$\delta g(r,\varphi,\lambda) = \frac{1}{r}\cdot\frac{GM}{R}\sum_{\ell=0}^{\ell\max}\left(\frac{R}{r}\right)^{\ell+1}(\ell+1) \times\sum_{m=0}^{\ell}\left[\delta\overline{C}_{\ell m}\cdot\cos(m\lambda)+\delta\overline{S}_{\ell m}\cdot\sin(m\lambda)\right]\cdot\overline{P}_{\ell m}(\sin\varphi) \tag{4}$$

The gravity variation δg_{load} induced by δr (Eq. 2) is:

$$\delta g_{\mathrm{load}} = \delta r\cdot\frac{\partial^2 W}{\partial r^2} \tag{5}$$

To calculate the second-derivative of the potential W with respect to the radius r, it is accurate enough to take only the zero degree term of Eq. (1). For $r = R$ we get:

$$\delta g_{\mathrm{load}}(r=R,\varphi,\lambda) = -2\frac{GM}{R^2}\cdot\delta N_\ell(\varphi,\lambda)\cdot h'_\ell \tag{6}$$

To compare the satellite-derived gravity variation with that measured by the SG, we add δg from Eq. (4) and δg_{load} from Eq. (6) and get with Eq. (3) at the Earth's surface ($r = R$):

$$\delta g_G(\varphi,\lambda) = \frac{GM}{R^2}\sum_{\ell=0}^{\ell\max}(\ell+1-2h'_\ell)\sum_{m=0}^{\ell}\left[\delta\bar{C}^G_{\ell m}\cdot\cos(m\lambda) +\delta\bar{S}^G_{\ell m}\cdot\sin(m\lambda)\right]\cdot\bar{P}_{\ell m}(\sin\varphi) \tag{7}$$

where the superscript G is related to spherical harmonic coefficients of GRACE gravity variations.

Based on Eqs. (1 – 7) it follows that taking the loading into account means multiplying the basic effect by degree-dependent scaling factors. Summing degrees 2 – 10 results in a loading effect that is almost proportional to the basic effect. The common scaling factor is about 1.35. Hence, the GRACE signal and the GRACE signal plus loading effect have almost the same form and no good or bad agreement between SG and GRACE can be introduced artificially.

The resulting monthly data sets of spherical harmonic coefficients have been used to calculate the gravity variations $\delta\mathrm{gm_G}$ (Eq. 7) for the selected SG positions in the time span from April 2002 to November 2003. According to Fig. 1, the coefficients are used from degree 2 through degrees 10, 15, and 20, which corresponds to a spatial resolution $\lambda/2 = 2{,}000$, 1,333 and 1,000 km, respectively.

4.2 SG gravity variations

The SG measures gravity variations associated with mass redistributions. According to the law of gravitation, the gravity sensor, a test mass, is sensitive to mass and distance changes. Therefore, the recordings include not only the tidal gravity from the Sun, Moon and other celestial bodies, but also the gravity effects induced by various geophysical and geodynamic sources on global, regional and local scales. The gravity variations induced by the atmosphere and hydrosphere contain the gravitational attraction part on the SG test mass and the deformation part of the Earth's surface. These gravity variations correlate with changes of atmospheric and hydrospheric parameters, such as atmospheric pressure, precipitation, groundwater table, soil moisture and sea level variations, which can be measured and used for modelling the gravity effects induced by the atmosphere and hydrosphere. Therefore, a separation and reduction from the raw gravity data is possible for these effects.

In a pre-processing procedure, spikes and steps due to instrumental and other perturbations, such as earthquakes, were carefully removed from the raw SG recordings. Spikes larger than 0.2 μgal and steps that do not have their origin in atmosphere- or groundwater level- induced gravity variations have been removed. Of special importance is the correction of steps in the raw data that are associated with instrumental problems (e.g. liquid Helium transfers or lightening strikes). This must be carried out with great care because steps in the data series directly influence the comparison results. Then, the data were low-pass filtered with a zero phase shift filter (corner period 300 s) and reduced to 1 h sampling rate. From these pre-processed gravity data (δg_{raw}), which include gravity variations of different sources, the same gravity effects are subtracted as in the GRACE data processing. These are:

- Earth tides: The Earth tide reduction is performed with the Wahr–Dehant model (e.g. Dehant (1987); Wenzel (1996)). The tidal parameters from this model were used for calculating the tidal gravity effect (*ET*) applied for semi-diurnal to long-periodic constituents (tidal frequencies 3.190895 – 0.00248 cpd).
- Gravity variations induced by the atmosphere (atmospheric pressure effect): For calculating the atmospheric pressure effect (δg_{air}), 3D atmospheric pressure data from ECMWF have been used. This gravity effect consists of both attraction and deformation part. The calculation of the attraction term is performed with the program 3DAP (Neumeyer et al. 2004b), which considers the real air density redistribution in the atmosphere. This result is more precise than the calculation with local or 2D atmospheric pressure data, because the surface pressure independent (SPI) part of the attraction term can only be determined with 3D data. The SPI part is of the order of up to 2 μgal at a seasonal period; therefore, it must be taken into account for comparing with GRACE-derived gravity variations. The deformation term is calculated according to the Green's function for atmospheric loading (Merriam 1992, Sun 1995).
- Ocean tidal loading: Based on the FES2002 global ocean tide model (Lefevre et al. 2002, Le Provost et al. 2002) the ocean loading for various waves in semi-diurnal, diurnal and long-periodic bands have been calculated with the GFZ program OCLO based on (Francis and Mazzega 1990). OCLO calculates the gravity variations induced by the ocean loading (δg_{ol}) in the time domain using data from FES2002. Because of the inaccuracy of the global

ocean tidal models, the lack of regional models and the complicated bay coastal lines, which induce a kind of special shallow sea tidal phenomena (Sun et al. 2002), additional tide gauge measurements can improve the ocean loading correction (Neumeyer et al. 2004c). This is recommended for SG stations near the ocean with a strong oceanic influence (Khan and Hoyer 2004).

- Pole tide (*PT*): The polar motion causes changes in centrifugal acceleration, which can be measured with the SG. From the IERS polar motion data $X_P(t)$ and $Y_P(t)$ (in terrestrial frame) the gravity effect of the polar motion can be calculated for the SG station with co-latitude θ and longitude λ according to Torge (1989)

$$\delta g_{\mathrm{Pol}}(\theta, \lambda, t) = R\omega^2 \delta_{\mathrm{Pol}} \sin(2\theta) \cdot [X_P(t)\cos(\lambda) - Y_P(t)\sin(\lambda)] \quad (8)$$

where R is the radius of a spherical Earth model, ω is the angular velocity of the Earth according to the IERS Conventions 2003 (McCarthy and Petit 2004) and $\delta_{\mathrm{Pol}} = 1.16$ is the gravimetric factor (Wahr 1985; Xu et al. 2004).

- Local groundwater level gravity effect (δg_{gwl}) induced by water circulation in the surroundings of the SG causes variation in the gravitational attraction and deformation at the surface similar to that due to the atmosphere. Precipitation causes changes in soil moisture and groundwater level. Presently, four of the SG stations used in this study are equipped with a borehole for measuring groundwater level variations. In many cases, a good correlation between gravity and groundwater level variations has been shown (Kroner 2001, Harnisch and Harnisch 2002; Virtanen 2001). The gravity effect of these variations is determined by regression analysis. The regression coefficient varies between 1 and 10 μgal/m depending on the hydrological conditions. This is a simple model that does not reflect the real hydrological gravity signal very accurately. Separating local from regional/global environmental signals is a challenge for interpreting temporal gravity variations. While suitable approaches exist for atmospheric signals (e.g. Boy et al. 2002, Neumeyer et al. 2004b) the problem is much more difficult and not yet satisfactorily solved when regarding hydrological signals. Both soil moisture and groundwater level data reflect local effects and also signals on regional or continental scale. Additionally, topography and local hydrological structure have a big impact on hydrological loading (e.g. Boy et al. 2005, Kroner and Jahr 2005, Meurers et al. 2005). All these facts restrict a clear separation of hydrological gravity contributions from different scales. In our study, we reduce the local hydrological gravity effect based on groundwater level variations near the SG station and we may also reduce a part of the global effect. For better modelling, a local hydrology model is necessary around the SG site, which considers the local hydrological cycle. Input data for this model should be precipitation, soil moisture and groundwater level variations measured at representative locations. With these data, modelling the local gravity variations induced by the hydrosphere can be better evaluated.
- The determination of the instrumental drift is based on polar motion measured by SG ($\delta g_{\mathrm{SG\_pol}} = \delta g_{\mathrm{raw}} - ET - \delta g_{\mathrm{air}} - \delta g_{\mathrm{ol}} - \delta g_{\mathrm{gwl}}$) and calculated from IERS data (*PT*). It is simulated by a first-order polynomial $dr(t) = a_0 + a_1 t$ and the drift parameters a_0 and a_1 are determined by a linear fit of $\delta g_{\mathrm{SG\_pol}}$ and *PT*.

After reduction of these gravity effects from the raw gravity data (Fig. 2), the remaining part can be assumed to be mainly mass changes in terrestrial water storage δg_{SG}.

$$\delta g_{\mathrm{SG}}(t) = \delta g_{\mathrm{raw}}(t) - ET(t) - PT(t) - \delta g_{\mathrm{air}}(t) - \delta g_{\mathrm{ol}}(t) - \delta g_{\mathrm{gwl}}(t) - dr(t) \quad (9)$$

From gravity variations δg_{SG}, monthly arithmetic means $\delta g m_{\mathrm{SG}}$ are calculated for comparison with GRACE (Fig. 3).

5 Gravity variations derived from global hydrology models

After reduction of different gravity effects from the SG recordings and the GRACE solutions, the remaining gravity variations are mainly induced by mass changes in continental water storage. Therefore, gravity variations were derived from global hydrology models for comparison with these "measured" hydrological effects (Wahr et al. 2004; Schmidt et al. (2005b)).

The aim of global hydrological models is to represent both the spatial distribution and the changes of continental water budget with time. Since every redistribution of water masses induces changes of the Earth's gravity field, the ideal hydrological model for our purposes should represent all water resources, available as ground water storage, in water basins, contained in ice shields or present in any other form. However, none of the existing models meet these requirements completely, and it is the purpose of the modern gravity missions to mitigate these inconsistencies.

Although the water budget change (wbc) of all global hydrological models is based on precipitation (prec), run-off (roff) and evapotranspiration (evpt), expressed by the very simple fundamental relation:

$$\mathrm{wbc} = \mathrm{prec} - \mathrm{roff} - \mathrm{evpt} \quad (10)$$

the implementation brings additional difficulties. There is no possibility to measure directly the water stocks, and the same holds – to some extent – for the remaining variable quantities. Hence, the possibilities to validate a model through a direct check of Eq. (10) using only the respective observables are very limited. Even in the case of strictly defined objective, the modelling freedom is rather large and two different models could be quite different, especially from the point of view of reflecting entirely the redistribution of water masses.

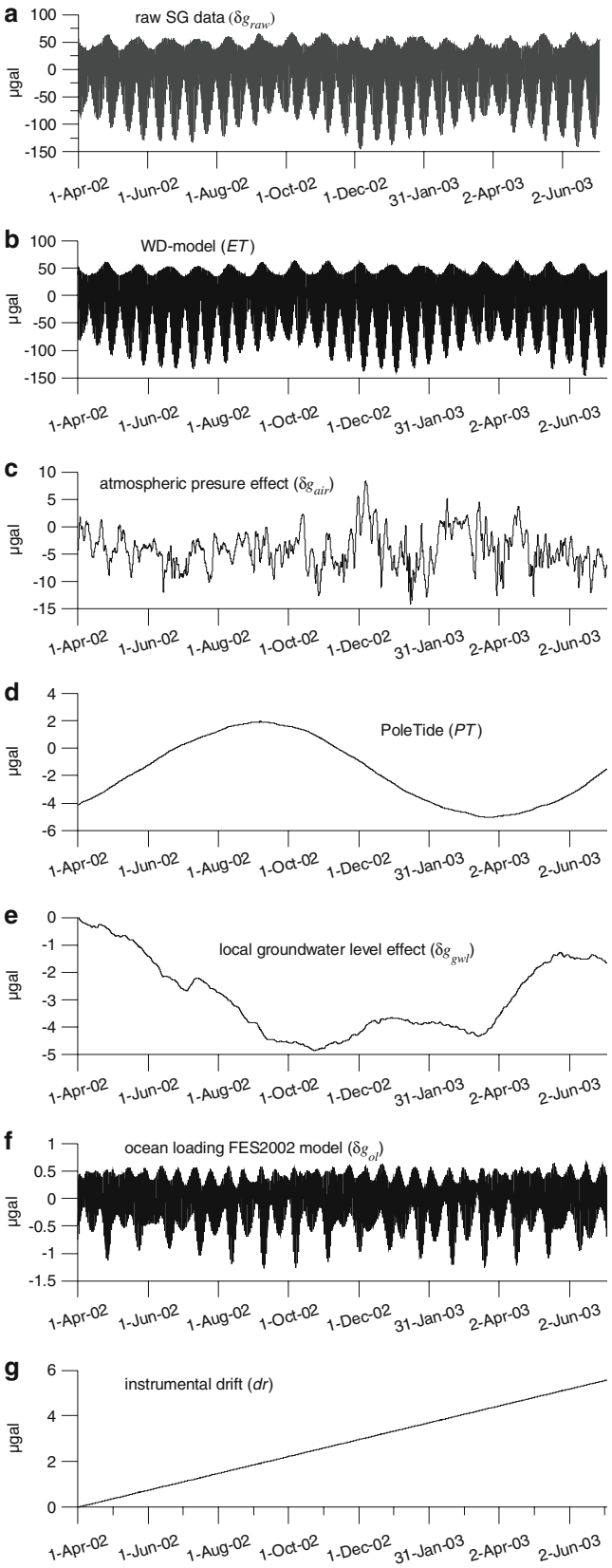

◄

Fig. 2 Reduction of the raw gravity data (Metsahovi station, Finland). **a** Raw gravity data (δg_{raw}). **b** Earth tides due to Wahr–Dehant-model (ET). **c** Atmospheric pressure effect (δg_{air}). **d** Pole tide (PT) due to International Earth Rotation Service (IERS) data. **e** Local groundwater level effect (δg_{gwl}). **f** Ocean loading due to FES2002-model (δg_{ol}). **g** Instrumental drift (*dr*)

5.1 Hydrology models considered

In the present study, three global hydrological models have been considered:

1. Water gap Global Hydrology Model (WGHM) (Döll et al. 2003), data coverage from 01/1992.
2. Leaky-Bucket Model (H96) (Huang et al. 1996, Fan and van den Dool 2004), data coverage from 01/1948.
3. Land Dynamics model (LaD) (Milly and Shmakin 2002), data coverage from 01/1980.

The output of these three models is available in the form of gridded data sets representing monthly averages of water storage expressed as equivalent water columns in mm or cm. The grid step in geographical latitude and longitude is 0.5° for the first two models and 1° for the third one. The models are updated regularly so that the current data are available with a delay of several months. It should be stressed that the depth of the considered groundwater in different models differs, the snow is taken into account only partially and in different ways, and the modelling of ice shields is, according to the authors, very incomplete and unreliable.

5.2 Computation of gravity variations from hydrological models

In order to compare the observed variations of the Earth's gravity field with the variations deduced from the changes in water storage as represented by global hydrological models, the component of the gravity field induced by the modelled water stocks have been computed for each epoch (i.e. month) and represented in spherical harmonics expansion with a GFZ analysis program based on Eq. (15).

The input data for each epoch are given on a regular geographical grid as equivalent water thickness $\delta h(\varphi, \lambda)$, which represents deviations from some reference state of the water budget in the considered block. Since $\delta h(\varphi, \lambda)$ does not represent some real water column, but an equivalent of complete water mass excess or deficit contained in groundwater, surface water, soil moisture and other considered components, it is reasonable to regard it as a surface mass using the relation:

$$\delta\sigma(\varphi, \lambda) = \rho_{\mathrm{W}}\delta h(\varphi, \lambda) \tag{11}$$

where ρ_{W} is the density of fresh water.

In order to compute gravitational effects, numerical integration of the surface mass density $\delta\sigma$ is necessary. According

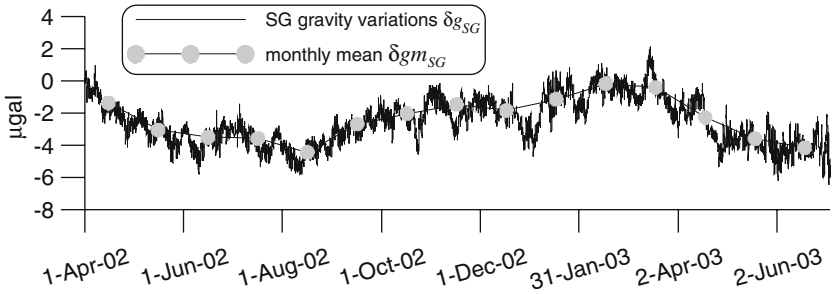

Fig. 3 Gravity variations δg_{SG} (*black line*) and δgm_{SG} (*grey dots*) for comparing with GRACE and hydrology models (Metsahovi station, Finland)

to Wahr et al. (1998), $\delta\sigma$ can be expanded as

$$\delta\sigma(\varphi,\lambda) = R\rho_W \sum_{\ell=0}^{\infty}\sum_{m=0}^{\ell} \bar{P}_{\ell m}(\sin\varphi)(\delta\hat{C}_{\ell m}\cos(m\lambda) + \delta\hat{S}_{\ell m}\sin(m\lambda)) \tag{12}$$

with

$$\begin{Bmatrix}\delta\hat{C}_{\ell m}\\ \delta\hat{S}_{\ell m}\end{Bmatrix} = \frac{1}{4\pi R\rho_W}\int_0^{2\pi} d\lambda \int_{-\pi/2}^{\pi/2} \sin\varphi d\varphi \delta\sigma(\varphi,\lambda) \times \bar{P}_{\ell m}(\sin\varphi)\begin{Bmatrix}\cos(m\lambda)\\ \sin(m\lambda)\end{Bmatrix} \tag{13}$$

Now it is possible to represent any gravitational effect as a sum of spherical harmonics by substituting $\delta\overline{C}_{\ell m}$ and $\delta\overline{S}_{\ell m}$ in Eqs. (1), (3) or (4), where

$$\begin{Bmatrix}\delta\overline{C}^{\mathrm{HM}}_{\ell m}\\ \delta\overline{S}^{\mathrm{HM}}_{\ell m}\end{Bmatrix} = \frac{3\rho_W}{\rho_{\mathrm{ave}}}\frac{1+k'}{2\ell+1}\begin{Bmatrix}\delta\hat{C}_{\ell m}\\ \delta\hat{S}_{\ell m}\end{Bmatrix} \tag{14}$$

and ρ_{ave} is the average mass-density of the Earth and k'_ℓ are loading Love numbers, which take into account the deformability of the solid Earth, that is the additional gravitational contribution resulting from the loading response. The superscript HM denotes spherical harmonic coefficients based on gravity variations derived from the hydrological model.

Of course, the variation δr of the radial position of the SG-station caused by the load must be considered as in the case of the GRACE-derived gravity variations. This can be done by applying Eq. (1) to Eq. (6). The equation for gravity variations derived from hydrological model δg_{HM} then takes the form:

$$\delta g_{\mathrm{HM}}(\varphi,\lambda) = \frac{GM}{R^2}\sum_{\ell=0}^{\ell_{\max}}(\ell+1-2h'_\ell) \sum_{m=0}^{\ell}\left[\delta\overline{C}^{\mathrm{HM}}_{\ell m}\cdot\cos(m\lambda) + \delta\overline{S}^{\mathrm{HM}}_{\ell m}\cdot\sin(m\lambda)\right]\cdot\overline{P}_{\ell m}(\sin\varphi) \tag{15}$$

for arbitrary $\ell_{\max}$, which is the same form as Eq. (7)

Degree-0 ($\ell = 0$) and degree-1 ($\ell = 1$) terms have not been used for the comparisons, since the hydrological models cannot and do not contain mass conservation, which does not exist on the level of continental water budget alone, and since hydrologically derived geocentre variations are not interpretable for the same reason.

5.3 Uncertainties of hydrological models

The main goal of this study is to compare temporal variations of the Earth's gravity field deduced from different sources. Prior to comparing variations deduced from global hydrological models with the respective variations resulting from GRACE or SG observations, it is necessary to get some feeling as to how reliably can this kind of information be deduced from global hydrological models. Global comparison of the variations of geoid undulations deduced from two different hydrological models shows differences that lie almost in the same order of magnitude as the variations themselves, although the correlation coefficients are rather high, see Table 2.

However, in some regions (e.g. the South American continent) the coincidence between the variability deduced from the three hydrological models is relatively good. The well-pronounced features, especially in large tropical river basins, are clearly visible in all three representations. In the context of the present paper, this means that the variations of the Earth's gravity field at some SG stations deduced from global hydrological models might be quite realistic. However, the existing global hydrological models in their present form still have to be regarded as rather uncertain. The main

Table 2 Weighted root mean-square (wrms) of the changes of geoid undulations (in mm) between different epochs deduced from H96, LaD and from differences H96-LaD as well as global correlation coefficients between H96 and LaD

	wrms			Corr.
Epochs	H96	LaD	H96-Lad	coeff.
05/2002 versus 08/2002	1.75	2.30	1.64	0.70
08/2002 versus 11/2002	0.66	1.12	0.77	0.74
11/2002 versus 03/2003	1.96	1.95	1.55	0.69
03/2003 versus 05/2003	0.47	1.05	0.87	0.58

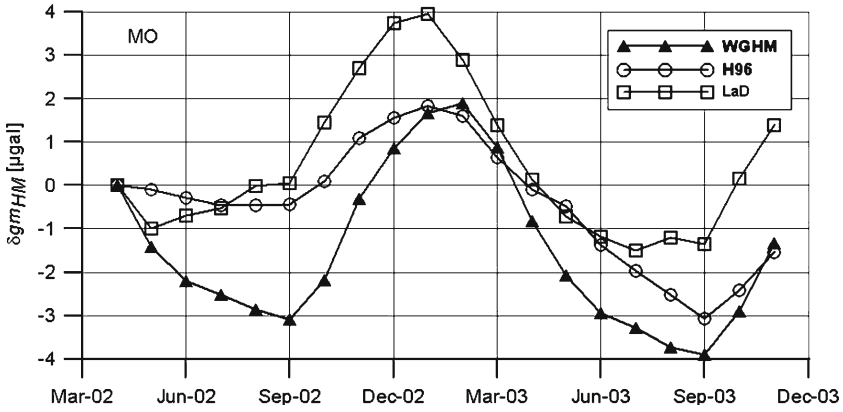

Fig. 4 Gravity variations derived from hydrology models WGHM, H96 and LaD (ℓ_{max}= 10) at the Moxa station, Germany

Table 3 Correlation between SG, GRACE (GFZ and UTCSR solutions) and hydrology model

	MO	WE	VI	ME	SU	WU	MA
$C_{SG-GFZ10}$	0.63	0.58	0.17	0.74	0.3	0.61	0.73
	(0.34)	(0.56)	–	(0.58)	(0.3)	-	-
$C_{SG-GFZ15}$	0.4	0.66	−0.22	0.45	−0.46	0.32	0.57
$C_{SG-GFZ20}$	0.13	0.65	−0.18	0.39	−0.42	0.49	−0.14
$C_{SG-CSR10}$	0.32	0.75	−0.21	0.74	0.54	0.45	0.44
$C_{SG-WGHM}$	0.74	0.67	−0.56	0.82	0.4	0.47	−0.13
C_{SG-H96}	0.52	0.84	−0.71	0.7	0.72	0.54	−0.5
C_{SG-LaD}	0.73	0.43	−0.47	0.89	0.38	0.45	0.5
$C_{GFZ10-WGHM}$	0.79	0.8	0.8	0.88	0.02	0.91	0.33
$C_{GFZ10-H96}$	0.52	0.61	0.7	0.8	0.75	0.94	−0.48
$C_{GFZ10-LaD}$	0.53	0.58	0.69	0.82	0.23	0.91	0.62

possibilities to validate these models in an independent way are comparisons with the gravity field determined either with satellite techniques, like GRACE (Schmidt et al. 2005a) or with SG, as in this study.

The deviations of the three models (Fig. 4) show the difficulties in modelling the gravity effect based on global hydrology models. A comparison between hydrology models, SG and GRACE gravity variations does not indicate any hydrology model that fits best everywhere. Depending on the SG location, one of the models matches SG and/or GRACE at best (Table 3; shown later).

6 Comparison of SG, GRACE and hydrology model-derived gravity variations

We did not select all possible stations available in the GGP SG network in this study, but rather focussed on selected sites with specific conditions (availability in the same time period, geographical distribution to sample different continental water storage cases, small noise level in the data).

Within the selected time period from April 2002 to November 2003, the SG gravity data from these sites were processed according to the procedure in Sect. 4.2. Only for the MO, WE and ME sites, the local groundwater level correction δg_{gwl} was performed. The measured groundwater level variations at the SU site are very small and show no correlation to the gravity signal. At the VI, WU and MA sites, no groundwater level data were available.

For comparison, the monthly averages of the gravity variations δgm_{SG} (Eq. 9) are used. The assigned GRACE values δgm_G are taken from the monthly global gravity field solutions calculated for the coordinates of the selected SG sites (Eq. 7). Because of the reduction due to Earth and ocean tides, pole tide and atmosphere, the remaining time variable gravity effects are mainly caused by continental large-scale hydrology. Eleven monthly solutions from GFZ and 14 solutions from UTCSR were available for the same period at ISDC of GFZ (http://isdc.gfz-potsdam.de/grace). For the SG sites, hydrology model-derived gravity variations δgm_{HM} (Eq.15) have also been calculated. Figure 5 summarizes the results. The error bars on the SG gravity (δgm_{SG}) do not represent measurement errors; they show the variations of gravity within the respective month.

In order to demonstrate the agreement of the different data series, the correlation coefficients between δgm_{SG} and δgm_{G_GFZ10} ($C_{SG-GFZ10}$), δgm_{G_GFZ15} ($C_{SG-GFZ15}$), δgm_{G_GFZ20} ($C_{SG-GFZ20}$), $\delta gm_{G\_UTCSR10}$ ($C_{SG-UTCSR10}$), δgm_{SG} and δgm_{HM_WGHM}($C_{SG-WGHM}$), δgm_{HM_H96} (C_{SG-H96}), δgm_{HM_LaD} (C_{SG-LaD}), δgm_{GFZ10} and δgm_{HM_WGHM} ($C_{GFZ10-WGHM}$), δgm_{HM_H96} ($C_{GFZ10-H96}$), δgm_{HM_LaD} ($C_{GFZ10-LaD}$) have been calculated (Table 3, in parentheses are correlation coefficients without groundwater level correction).

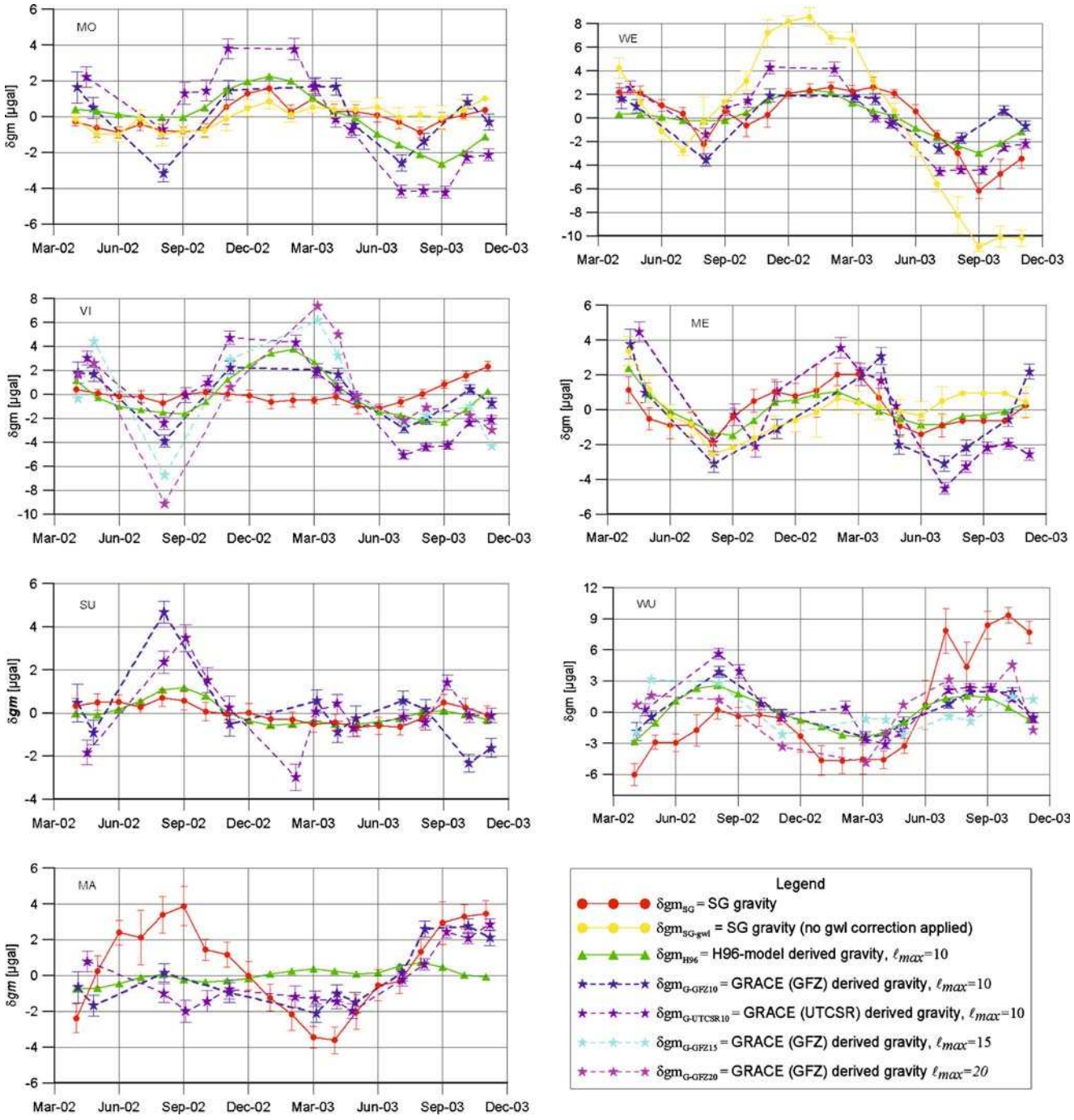

Fig. 5 Gravity variations from SG, GRACE and H96-model (δgm) at SG sites MO, WE, VI, ME, SU, WU, MA

It should be taken into account that the correlation computation is based on 11 (GFZ solution) or 14 (UTCSR solution) data points only, meaning that the degree of freedom can be at most 14 (in statistical applications of the correlation, degree of freedom of several hundreds is no exception). Hence, the computed values of the correlation coefficient should be considered as rather insignificant in a statistical sense. However, they give an objective measure of how similar the two curves look (opposed to a subjective estimate of a viewer). Further, it should not be forgotten that the correlation compares only the forms, giving no information about the relation of magnitudes. Such an approach is legitimate, since the scale of some of the models used for physical quantities is rather uncertain. This holds in the first place for global hydrology models, Sect. 5.3 and especially Table 2.

For all SG locations, the GRACE solutions of GFZ $\delta gm_{\mathrm{GGF710}}$ and UTCSR $\delta gm_{\mathrm{GUTCSR10}}$ are relatively close to each other. Differences may be caused by different processing procedures (see Sect. 4.1). The agreement between GRACE, SG and hydrological model-derived gravity variations is different depending on the site. This expresses the uncertainties of all three data series.

According to Table 3, the correlation coefficients between δgm_{SG} and δgm_{G} lie above the level of 0.5 for all SG sites except VI, $C_{\mathrm{SG-GFZ10}}$ for the stations MO, WE, ME, WU and MA and $C_{\mathrm{SG-UTCSR10}}$ for WE, ME and SU. However, the correlation coefficients $C_{\mathrm{SG-GFZ10}}$ are small for VI and SU or $C_{\mathrm{SG-UTCSR10}}$ for MO, WU. Of all SG sites, VI has the lowest correlation for the GFZ and a negative correlation for the UTCSR solution. This may be caused by an unconsidered hydrological signal or an SG instrumental problem. Therefore, the data for this station are not suitable for comparison at present. The low correlation for the SU station is mostly caused by the large gravity signals in August 02 ($\delta gm_{\mathrm{G-GFZ10}}$) and September 2002 and February 2003 ($\delta gm_{\mathrm{G-UTCSR10}}$). The reason for this is unknown.

For the MO station, the SG data are also corrected for groundwater level changes. However, we could not consider a hydrological portion caused by rainfall and changing soil moisture above the SG, because the site is located in a mountain tunnel. This portion may influence the reduction of the hydrological signal (Kroner 2001).

The effect of the local groundwater level reduction is shown for MO, WE and ME (Fig. 5 yellow curves). SG variations are far too large without reduction of the groundwater level effect δg_{gwl} for WE. After reduction of δg_{gwl} there is a better agreement ($C_{\mathrm{SG-GFZ10}} = 0.58$, $C_{\mathrm{SG-UTCSR10}} = 0.75$, $C_{\mathrm{SG-H96}} = 0.84$). All data series match each other well. For ME and MO, we also obtain a better agreement with the gravity variations from GRACE and hydrological models after reduction of the groundwater level changes and also the correlation coefficients become higher (Table 3). For SU, this influence is negligible. The SG gravity variations at WU and MA are larger than those of GRACE and a hydrology model. Groundwater level variations, which were not available, are suspected as a possible cause for this.

The correlation of SG and hydrological models are different depending on the model. The best fits are at MO location for WGHM; WE, SU and WU locations for H96; ME and MA locations for LaD. Correlations between SG and best-fitted hydrological models are higher than those of SG and GRACE for MO, WE, ME and SU. We got similar results for the correlation of GRACE and hydrological models.

According to Sect. 2 the spherical harmonic coefficients have been calculated up to ℓ_{max}=10 for the GRACE solutions. In Fig. 5, ℓmax is increased to 15 (1,330 km) and 20 (1,000 km) for VI and WU. For ℓ_{max} =15 an agreement is still present, while for ℓ_{max}=20 the deviations become larger. The correlation coefficients $C_{\mathrm{SG-GFZ15}}$ and $C_{\mathrm{SG-GFZ20}}$ are smaller than $C_{\mathrm{SG-GFZ10}}$ (Table 3) and they lie just above the 0.5 level for WE (ℓ_{max} =15 and 20) and MA (ℓ_{max} =15). From this results it follows that the GRACE solution delivers the best result for comparison with SG measurements at ℓ_{max}= 10 – 15 (Fig. 1).

7 Conclusions

Our comparison shows quite a good agreement among SG, GRACE and hydrology model-derived gravity variations; within their estimated error limits for most of the selected SG locations. The individual discrepancies may give suggestions for further investigations of each data series.

For improving the combination of the different data sets, the following recommendations can be given:

- All SG sites should be equipped with groundwater table, soil moisture and rain gauges for better modelling of the local hydrological gravity effect;
- For each SG station, a local hydrology model based on real data should be developed;
- Only SG sites where the local hydrological gravity effects can be well modelled are recommended for validation of GRACE and global hydrology models.

For further validation experiments, field SG measurements should be carried out in areas with large or very small gravity variations, for example the Amazon area in South America, where seasonal gravity changes can be observed in the order of some 10 μgal or in the Atacama desert (Chile) where only a very weak hydrology signal is to be expected.

The deviations of the different data sets cannot presently be explained completely. There are still open questions, for example, why gravity variations derived from global hydrology models do not fit to SG and GRACE results for the Matsushiro site? What happened on August 2002 to the GRACE solution at Sutherland site? To answer these questions in full, investigations on longer data sets are necessary.

Acknowledgements The authors thank Chris Milly of the US Geological Survey, USA, Yun Fan and Huug van den Dool of the Climate Prediction Center (National Oceanographic and Atmospheric Administration), USA, as well as Petra Döll of University Frankfurt aM., Germany, and Andreas Güntner of GFZ Potsdam, Germany, for providing the LaD, H96 and WGHM data, respectively. The German Ministry of Education and Research (BMBF) supports the GRACE project within the GEOTECHNOLOGIEN geoscientific R&D program under grant 03F0326A.

References

Ali AH, Zlotnicki V (2003) Quality of wind stress fields measured by the skill of a barotropic ocean model: importance of stability of the marine atmospheric boundary layer. Geophys Res Lett 30(3):1129, doi: 10.1029/2002GL016058

Boy JP, Gegout P, Hinderer J (2002) Reduction of surface gravity data from global atmospheric pressure loading. Geophys J Int 149:534–545

Boy JP, Hinderer J, Ferhat G (2005) Gravity changes and crustal deformation due to hydrology loading. Geophys Res Abstracts 7:07166

Bettadpur S (2004) UTCSR Level-2 processing standards document. GRACE 327–742, http://isdc.gfz-potsdam.de or http://podaac.jpl.nasa.gov/grace/
Bulletin B http://www.iers.org/iers/products/eop/monthly.html
Chen JL, Wilson CR, Tapley BD, Ries JC (2004) Low degree gravitational changes from GRACE: validation and interpretation, Geophys Res Lett 31:L22607, doi:10.1029/2004GL021670
Cheng MK, Shum CK, Tapley BD (1997) Determination of long-term changes in the Earth's gravity field from satellite laser ranging observations. J Geophys Res 102:22377–22390
Crossley D, Hinderer J, Casula O, Francis O, Hsu HT, Imanishi Y, Jentzsch G, Kääriäinen J, Merriam J, Meurers B, Neumeyer J, Richter B, Sato D, Shihuya K, van Dam T (1999) Network of superconducting gravimeters benefits a number of disciplines. EOS Trans Am Geoph Union 80(11):125–126
Crossley D, Hinderer J (2002) GGP ground truth for satellite missions. Bull Inf Marees Terrestres 136:10735–10742
Crossley D, Hinderer J, Llubes M, Florsch N (2003) The potential of ground gravity measurements to validate GRACE data. Adv Geosci 1:1–7
Crossley D, Hinderer J, Boy JP (2005) Time variation of the European gravity field from superconducting gravimeters. Geophys J Int 161:257–264, doi:10.1111/j.1365–246X.2005.02586.x
Desai SD (2002) Observing the pole tide with satellite altimetry. J Geophys Res 107 (C11):3186, doi:10.1029/2001JC001224
Dehant V (1987) Tidal parameters for an inelastic earth. Phys Earth Planet Int 49:97–116
Dunn C, Bertiger W, Bar-Sever Y, Desai S, Haines B, Kuang D, Franklin G, Harris I, Kruizinga G, Meehan T, Nandi S, Nguyen D, Rogstad T, Brooks Thomas JB, Tien J, Romans L, Watkins M, Wu S-C, Bettadpur S, Kim J (2003) Instrument of GRACE – GPS augments gravity measurements. GPS World 14(2):16–28
Döll P, Kaspar F, Lehner B (2003) A global hydrological model for deriving water availability indicators: model tuning and validation. J Hydrol 270:105–134
Fan Y, van den Dool H (2004) The CPC global monthly soil moisture data set at 1/2 degree resolution for 1948-present. J Geophys Res 109:D10102, doi:1029/2003JD004345
Farrell WE (1972) Deformation of the Earth by surface loads. Rev Geophys Space Phys 10:761–797
Flechtner F (2003a) GFZ level-2 processing standards document. GRACE 327–743, http://isdc.gfz-potsdam.de or http://podaac.jpl.nasa.gov/grace/
Flechtner F (2003b) AOD1B product description document. GRACE Project Documentation. JPL 327–750, Rev 1.0, JPL Pasadena, Ca. http://podaac.jpl.nasa.gov/grace/daac/doc/AOD1B_20031022.pdf
Francis O, Mazzega P (1990) Global charts of ocean tide loading effects. J Geophys Res 95:11411−11424
Goodkind J M (1999) The Superconducting gravimeter. Rev Sci Instrum 70/11:4131–4152
Han SC, Jekeli C, Shum CK (2004) Time-variable aliasing effects of ocean tides, atmosphere, and continental water mass on monthly mean GRACE gravity field. J Geophys Res 109:B 04403, doi:10.1029/2003/JB002501
Harnisch G, Harnisch M (2002) Seasonal variations of hydrological influences on gravity measurements at Wettzell. Bull D'Inf Marees Terr 137:10849–10861
Heiskanen WA, Moritz H (1967) Physical geodesy. WH Freeman, San Francisco
Hinderer J, Legros H (1989) Elasto – gravitational deformation, relative gravity changes and Earth dynamics. Geophys J Int 97: 481–495
Huang J, Van den Dool HM, Georgakakos KP (1996) Analysis of model-calculated soil moisture over the United States (1931–1993) and applications to long-range temperature forecasts. J Climate 9:1350–1362
Khan SA, Hoyer J (2004) Shallow-water tides in Japan from superconducting gravimetry. J Geod 78:245–250
Kroner C (2001) Hydrological effects on gravity data of the Geodynamic Observatory Moxa. J Geodyn Soc Jpn 47(1):353–358
Kroner C, Jahr T (2005) Hydrological experiments around the superconducting gravimeter at Moxa observatory. J Geodyn (accepted)
Lefevre F, Lyard FH, Le Provost C, Schrama EJO (2002) FES99: a global tide finite element solution assimilating tide gauge and altimetric information, J Atmos Oceanic Technol 19:1345–1356
Le Provost C, Lyard F, Lefevre F, Roblou L (2002) FES 2002 – A new version of the FES tidal solution series. Abstract Volume Jason-1 Science Working Team Meeting, Biarritz, France
Lyard F (1998) Long period tides determination from a hydrodynamic and assimilation tidal model. Study Report, GeoForschungsZentrum Potsdam
McCarthy D, Petit G (2004) IERS Conventions (2003). IERS Technical Note 32, IERS Central Bureau, Frankfurt a.M., Germany
Meurers B, Van Camp M, Petermans T, Verbeeck K, Vanneste K (2005) Investigation of local atmospheric and hydrological gravity signals in Superconducting Gravimeter time series. Geophys Res Abstracts 7:07463
Merriam J B (1992) Atmospheric pressure and gravity. Geophys J Int 109:488–500
Milly PCD, Shmakin AB (2002) Global modelling of land water and energy balances. Part I: The land dynamics (LaD) model, J Hydrometeorol 3(3):283–299
Neumeyer J, Schwintzer P, Barthelmes F, Dierks O, Imanishi Y, Kroner C, Meurers B, Sun HP, Virtanen H (2004a) Comparison of superconducting gravimeter and CHAMP satellite derived temporal gravity variations. In: Reigber Ch, Lühr H, Schwintzer P, Wickert J (eds) Earth observations with CHAMP: Results from three years in orbit, pp 31–36
Neumeyer J, Hagedoorn J, Leitloff J, Schmidt T (2004b) Gravity reduction with three-dimensional atmospheric pressure data for precise ground gravity measurements. J Geodyn 38:437–450
Neumeyer J; del Pino J; Dierks O, Pflug H (2004c) Improvement of ocean loading correction on gravity data with additional tide gauge measurements. J Geodyn 40:104–111
Pick M. Picha J. Vyskocil V (1973) Theory of the Earth's gravity field. Publishing House of the Czechoslovak Academy of Sciences, Prague
Reigber Ch, Schmidt R, Flechtner F, König R, Meyer U, Neumayer KH, Schwintzer P, Zhu S Y (2005) An Earth gravity field model complete to degree and order 150 from GRACE: EIGEN-GRACE02S. J Geodyn 39:1–10
Rosat S, Hinderer J, Crossley D, Boy JP (2004) Performance of superconducting gravimeters from long-period seismology to tides. J Geodyn 38:461–476
Schmidt R, Flechtner F, Meyer Ul, Reigber Ch, Barthelmes F, Foerste Ch, Stubenvoll R, König R, Neumayer KH, Zhu SY (2005a) Static and time-variable gravity from GRACE Mission Data. In: Rummel R, Reigber Ch, Rothacher M, Boedecker G, Schreiber U, Flury J (eds) Observation of the Earth system from space, Springer, Berlin Heidelberg New York (in preparation)
Schmidt R, Schwintzer P, Flechtner F, Reigber Ch, Güntner A, Döll P, Ramillien G, Cazenave A, Petrovic S, Jochmann H, Wünsch J (2005b) GRACE Observations of Changes in Continental Water Storage. Global and Planetary Change 48/4:259–273
Sun H-P (1995) Static deformation and gravity changes at the Earth's surface due to the atmospheric pressure. Observatoire Royal des Belgique, Serie Geophysique Hors-Serie, Bruxelles
Sun H-P, Hsu H-T, Jentzsch G, Xu J-Q (2002) Tidal gravity observations obtained with superconducting gravimeter and its application to geodynamics at Wuhan/China, J Geodyn 33(1–2):187–198
Tapley BD, Reigber Ch (2001) The GRACE mission: status and future plans. EOS Trans AGU 82 (47), Fall Meet Suppl G41:C-02
Thompson PF, Bettadpur SV, Tapley BD (2004) Impact of short period, non-tidal, temporal mass variability on GRACE gravity anomalies. Geophys Res Lett 31:L06619, doi:10.1029/2003GL019285
Torge W (1989) Gravimetry, de Gruyter, Berlin, New York
Vaníček P, Krakiwsky EJ (1982) Geodesy: the Concepts. North -Holland, Amsterdam, New York, Oxford
Virtanen H (2001) Hydrological studies at the gravity station Metshovi, Finland. J Geodetic Soc Jpn 47(1):328–333

Wahr J, Molenaar M, Bryan F (1998) Time variability of the Earth's gravity field: Hydrological and oceanic effects and their possible detection using GRACE. J Geophys Res 103(12):30205–30229

Wahr J (1985) Deformation induced by polar motion. J Geophys Res 90(B11):9363–9368

Wahr J, Swenson S, Zlotnicki V, Velicogna I (2004) Time-variable gravity from GRACE: First results. Geophys Res Lett 31(11):L11501, doi:10.1029/2004GL019779

Wenzel HG (1996) The nanogal software: data processing package Eterna 3.3. Bull Inf Marees Terrestres 124:9425∼9439

Xu JQ, Sun HP, Yang XF (2004) A study of gravity variations caused by polar motion using superconducting gravimeter data from the GGP network. J Geod 78:201–209

Zürn W, Wilhelm H (1984) Tides of the Earth. In Landolt-Börnstein, Springer, Berlin Heidelberg New York Tokyo, vol 2, pp 259–299